Pharm Res (2014) 31:635–648
DOI 10.1007/s11095-013-1185-2

RESEARCH PAPER

Quantitative Analysis of Target Coverage and Germinal Center Response by a CXCL13 Neutralizing Antibody in a T-Dependent Mouse Immunization Model

Joanne Brodfuehrer • Andrew Rankin • Jason Edmonds • Sean Keegan • Tatyana Andreyeva • Rosemary Lawrence-Henderson • Josef Ozer • Huilan Gao • Laird Bloom • Angela Boisvert • Khetemenee Lam • Julie Lee • Timothy LaBranche • Jameel Syed • Wenyan Miao • Pratap Singh

Received: 12 May 2013 / Accepted: 9 August 2013 / Published online: 5 November 2013

ABSTRACT

Purpose Study the impact of CXCL13 neutralization on germinal center (GC) response *in vivo*, and build quantitative relationship between target coverage and pharmacological effects at the target tissue.

Methods An anti-CXCL13 neutralizing monoclonal antibody was dosed *in vivo* in a T-dependent mouse immunization (TDI) model. A quantitative site-of-action (SoA) model was developed to integrate antibody PK and total CXCL13 levels in serum and spleen towards estimating target coverage as a function of dose. To aid in the SoA model development, a radio-labeled study using [I^{125}] CXCL13 was conducted in mice. Model estimated target coverage was linked to germinal center response using a sigmoidal inhibitory effect model.

Results *In vivo* studies demonstrated that CXCL13 inhibition led to an architectural change in B-cell follicles, dislocation of GCs and a significant reduction in the GC absolute numbers per square area (GC/mm^2). The SoA modeling analysis indicated that ~79% coverage in spleen was required to achieve 50% suppression of GC/mm^2. The 3 mg/kg dose with 52% spleen coverage resulted in no PD suppression, whereas 30 mg/kg with 93% coverage achieved close to maximum PD suppression, highlighting the steepness of PD response.

Conclusions This study showcases an application of SoA modeling towards a quantitative understanding of CXCL13 pharmacology.

KEY WORDS CXCL13 · germinal centers · modeling PK/PD · site-of-action

ABBREVIATIONS

CXCL13	CXC chemokine 13
ELISA	Enzyme-linked immunosorbent assay
GC	Germinal center
GC/mm^2	Germinal centers per mm^2
PD	Pharmacodynamics
PK	Pharmacokinetics
SoA	Site of action
TDI	T-dependent immunization model

INTRODUCTION

The chemokine CXCL13 is constitutively expressed in secondary lymphoid tissues by stromal cells such as follicular dendritic cells (FDCs), where it contributes to lymphorganogenesis as well as to regulating antibody responses (1,2). CXCR5, the lone receptor for CXCL13, is expressed by B cells and a subset of $CD4^+$ T cells termed T follicular helper

Electronic supplementary material The online version of this article (doi:10.1007/s11095-013-1185-2) contains supplementary material, which is available to authorized users.

J. Brodfuehrer · R. Lawrence-Henderson · J. Ozer · P. Singh
Department of Pharmacokinetics, Dynamics and Metabolism
Pfizer Inc., Cambridge, Massachusetts, USA

A. Rankin · J. Edmonds · S. Keegan · T. Andreyeva · J. Lee · W. Miao
Department of Immunology and Autoimmunity Pfizer Inc.
Cambridge, Massachusetts, USA

H. Gao · L. Bloom · A. Boisvert · K. Lam
Department of Global Biotherapeutics Technologies
Pfizer Inc., Cambridge, Massachusetts, USA

T. LaBranche · J. Syed
Department of Drug Safety R&D Pfizer Inc.
Cambridge, Massachusetts, USA

P. Singh (✉)
35 Cambridgepark Drive, Cambridge, Massachusetts 02140, USA
e-mail: pratap.singh@pfizer.com

(T_{FH}) cells that are critical for driving T cell-dependent antibody responses (3,4). Mice deficient in either CXCL13 or its receptor have a near-complete absence of lymph nodes (1). In spleen, CXCL13-deficient animals exhibit altered lymphoid architecture with a loss of interfollicular regions and disorganized distribution of marginal zone and follicular B cells around the T cell-rich area of the periarteriole lymphoid sheath (PALS) (1).

Further, CXCL13 along with CXCR5 regulates germinal center formation in secondary lymphoid tissues during an immune response. Upon challenge with a T-dependent antigen, highly specialized microanatomical structures termed germinal centers form within B cell follicles and contain follicular dendritic cells, T_{FH} cells and antigen-specific B cells. Germinal centers provide the optimal microenvironment for maintenance of B cell activation, somatic hypermutation, class switching and ultimately differentiation into high-affinity antibody-secreting plasma cells. In CXCL13 deficient mice, germinal centers were mis-localized to the T cell zone and appeared smaller (1).

In humans, aberrant CXCL13 expression has been observed in inflamed tissues of patients with various autoimmune diseases such as rheumatoid arthritis (RA), systemic lupus erythematosus (SLE), multiple sclerosis (MS), and Sjögren's syndrome (5–8). The expression of CXCL13 is often associated with leukocyte infiltration and the development of tertiary lymphoid structures in the tissues (5,8–10). Consistent with its role in chemotaxis, the tissue levels of CXCL13 have been reported to be many-fold higher at the sites of inflammation when compared to the circulating levels in serum in these diseases. For example, recent data obtained from the 14 RA patients indicate that the average CXCL13 levels in synovial fluids were 5-fold higher than the serum concentrations (10,11).

Available experimental data as described above support the rationale for targeting CXCL13 for the treatment of the autoimmune diseases with leukocyte tissue infiltration and/or germinal center involvement. However, it remains unclear whether blockade of CXCL13 in established disease will provide benefit in post-developmental animals and in established immune response in humans. Recently, a CXCL13 neutralizing antibody dosed at 5 mg/kg to a mouse model of arthritis showed improvement in arthritis score but the exact mechanism for the improvement in disease activities remained unclear (12). Authors showed that the antibody dosing disrupted splenic follicles but the tertiary follicles in synovium or the salivary gland in immunized mice were largely unaffected. Since modulation of CXCL13 levels were not studied in serum or the tissues of interest, it was unclear from the results whether adequate neutralization of CXCL13 was achieved at 5 mg/kg dose. Moreover, a dose–response analysis was not conducted in this study, thus dose dependent effects on the disease activity and GC response could not be illustrated.

Given the potential of CXCL13 neutralization as a new paradigm for the treatment of autoimmune disease, it is important to understand the exposure-response relationship of CXCL13 neutralization using *in vivo* models. Further, target modulation at the level of serum and the target tissues of interest needs to be studied in order to determine the level of target coverage that is required for significant effect on CXCL13 pharmacology. To this end, we studied the effects of a mouse CXCL13 neutralizing antibody, HG1-2, in a T-dependent immunization model (TDI) using single- and multiple-dose studies (Table I). First, a single dose study at 10 mg/kg level was conducted in immunized mice and full PK/PD time course was obtained to establish the kinetic link and estimate parameters related to the antibody exposures and the resulting increase in total CXCL13 in serum and target tissue (i.e. spleen). Secondly, pharmacological impact of anti-CXCL13 treatment on the spleen B cell follicle architecture and germinal centers was assessed at 3, 10 and 30 mg/kg in the 10-day multiple-dose study. The experimental data obtained from these studies, i.e. pharmacokinetic (PK), total CXCL13 levels in serum/spleen, and PD data (i.e. GC response) was integrated using a quantitative site-of-action (SoA) model. To aid the quantitative model development, a radiolabeled study with [I^{125}]-CXCL13 was conducted in mice to determine *in vivo* turnover rate of CXCL13. As described below, a combination of experimental and quantitative modeling approach was developed to establish a relationship between target coverage at the site-of-action (i.e. spleen) and resulting PD response.

Table I Details of *In Vivo* Studies in Mice

Study	Dosing regimen	Study end points	Study objective
Single-dose TDI	10 mg/kg HG1-2 single dose (i.p.)	Serum and spleen samples at 1, 6, 24, 30, 48, 72, 96, 120 and 168 h.	To estimate key parameters for site-of-action model (Fig. 1).
Multiple- dose TDI	3, 10, 30 mg/kg HG1-2 (i.p.) 3 doses every 72 h	Serum: 6 h post 1st dose, 24 & 72 h post 3rd dose. Spleens: 11 days post 1st dose	Germinal center dose response, and limited serum PK/PD data to estimate target coverage after multiple doses of HG1-2.
Radio-labeled CXCL13 Study	I^{125}-CXCL13 (0.5 mCi) single i.v. bolus dose	TCA-precipitable radioactive counts in plasma at multiple timepoints	Determination CXCL13 *in vivo* half-life and corresponding *Kdeg* parameter (Fig. 1).

TDI T-dependent immunization model

MATERIALS AND METHODS

Animals

Six to eight week old female C57Bl/6 mice were obtained from Taconic for the pharmacokinetic and immunization studies. All animals were housed in a pathogen-free animal facility at Pfizer. Mice were between 8 and 12 weeks of age at the time of immunization. The *in vivo* mouse pharmacokinetic animal use protocol was approved by the Pfizer Cambridge Andover Institutional Animal Care and Use Committee (IACUC), and complies with the Association for Assessment and Accreditation of Laboratory Animal Care Internationally guidelines (AAALAC). The radiolabeled [I^{125}] experiments were conducted in male DBA mice and followed the Pfizer Radiation Safety Committee and Officer guidelines in compliance with Massachusetts and US law for radioisotope use.

Single and Multiple Dose Studies in T-dependent Immunization Model

Mice were immunized i.p. with 100 μg 4-hydroxy-3-nitrophenylacetyl-chicken γ globulin (NP-CGG; Biosearch Technologies, Novato, CA) emulsified in CFA (MP Biomedicals, Solon, OH). As summarized in Table I, in single dose studies, mice ($N=4$) were injected with 10 mg/kg i.p. dose of HG1-2 post-immunization. Serum and spleen tissues were collected at 1, 6, 24, 30, 48, 72, 96, 120, 168 h post antibody dose. In multiple dose studies, mice ($N=9$) were injected i.p. with 3 doses of HG1-2 or the control IgG twice a week (every 72 h) starting 1 day before the induction of immunization. Serum samples were collected at following time points: 6 h after the first dose, 24 h and 72 h after the third dose. Spleens were harvested 10 days post immunization.

Spleen Germinal Center Immunohistochemistry and Quantitation

Immunohistochemical staining for IgD (clone 11-26c.2a; BD Biosciences) and biotinylated peanut agglutinin (PNA; Vector Labs, Burlingame, CA) was performed using acetone-fixed cryosections of spleen specimens. TBST (DakoCytomation, Denmark) was used for washes between each step. Endogenous peroxidases were quenched with Dako Dual Endogenous Enzyme-Blocking Reagent (DakoCytomation, Denmark) for 10 min according to the manufacturer's directions. A protein block (TBST and 10% bovine serum) was applied for 30 min to the sections. IgD and PNA staining were performed at 1 and 4 μg/ml, respectively, in TBST plus 10% bovine serum. Streptavidin:HRP (eBioscience, San Diego, CA) was incubated with PNA-stained sections prior to development. IgD staining was detected with Rat-on-Mouse-AP-Polymer (BioCare Medical, Concord, CA). Diaminobenzidine substrate chromogen (DakoCytomation) was applied to HRP-labeled sections, and Permanent Red Chromagen (DakoCytomation) was applied for alkaline phosphatase-labeled sections. Sections were then rinsed in water and cover-slipped.

Antibody Expression and Purification

Anti-mouse CXCL13 neutralizing antibody, HG1-2, was produced by grafting the variable regions from published sequences of a mouse anti-mouse CXCL13 monoclonal antibody (U.S. Patent Application US 2008/0227704 A1, pub. date Sep. 18, 2008) (13) onto mouse IgG1 and kappa constant domains. Vectors expressing HG1-2 mIgG1 heavy and light chains were stably co-transfected into Chinese hamster ovary (CHO) cells. Conditioned medium was filtered through a polypropylene 5 μm/0.2 μm membrane (PALL, USA) and purified on a Protein A FF Sepharose column (GE Healthcare, Pittsburgh, PA, USA) pre-equilibrated with PBS-CMF (137 mM NaCl, 2.7 mM KCl, 8.1 mM Na_2HPO_4, 2.7 mM KH_2PO_4, pH 7.2) at a flow rate of 10 ml/min on an ÄKTAExplorer (GE Healthcare, Piscataway, NJ, USA). After washing with ten additional column volumes of PBS-CMF, the antibody was eluted with 20 mM citric acid, 150 mM NaCl, pH 2.5 and immediately neutralized with 5–10% 2 M Tris pH 8.0. The eluate was then subjected to gel filtration (Superdex-200, GE Healthcare, USA) in PBS-CMF to achieve a final purity above 99% and further concentrated using a Vivaflow 50 concentrator following the manufacturer's instructions (Sartorius stedim biotech, Goettingen, Germany).

Antibody Affinity Using BIAcore Assay

The HG1-2 antibody was captured *via* directly immobilized anti-murine IgG onto a carboxymethylcellulose sensor chip surface (CM5) in a BIAcore T100 instrument (GE Healthcare, Fairfield, CT). Various concentrations of murine CXCL13 (R&D Systems, Minneapolis, MN) in PBS-NET were injected for a 3 min. association at 100 μl/min. and allowed to dissociate for 20–60 min. At the end of each cycle, the anti-IgG surface was regenerated by a 30 s pulse of 10 mM Glycine HCl pH1.7 followed by two consecutive 15-s pulses of PBS-NET. All injections were performed in triplicate at 25°C at a collection rate of 10 Hz. For each analysis, sensorgrams were double referenced using a blank reference surface and by subtracting the average of several buffer injections. Rate constants were determined by fitting the data to a 1:1 model in BIAevaluation software v4.1.1 and the equation $K_D = k_{off}/k_{on}$. Theoretical Rmax was calculated as follows: molecular weight of analyte/ molecular weight of ligand × captured level of ligand (RU) × apparent stoichiometry (two moles of mCXCL13 bound per mole of HG1-2 antibody).

Antibody Affinity Using Serum ELISA

The HG1-2 binding affinity to the endogenous CXCL13 was determined using C57Bl/6 mouse serum (sex unknown). HG1-2 was serially diluted in R&D Systems Calibrator Diluent RD5-3 (R&D systems, Minneapolis, MN, 895436). Mouse serum was then mixed with an equal volume of serially diluted HG1-2 and incubated at ambient temperature for 30 min. Samples and standards were added to the ELISA plate, and incubated for 15 min shaking at ambient temperature. The protocol provided with the Quantikine mouse CXCL13/BLC/BCA-1 immunoassay kit (R&D systems, Minneapolis, MN, MCX130) was followed for the remainder of the assay. Free CXCL13 levels were calculated with a standard curve generated with recombinant CXCL13 (R&D systems, Minneapolis, MN). Finally, the free CXCL13 and HG1-2 concentrations were fit to a binding equilibrium equation ("Data Analysis and Fitting" section) to estimate binding affinity constant.

CXCL13 Chemotaxis Assay

Ba/F3/mCXCR5 cell line stably over-expressing mouse CXCR5 was generated and maintained at 37°C, 5% CO_2 in RPMI 1640 plus 10% heat inactivated fetal calf serum, 0.75ug/ml puromycin and 2 ng/ml recombinant mouse IL-3 (R&D systems, Minneapolis, MN, 403-ML). Chemotaxis assays were performed with the NeuroProbe chemotaxis plates with 8 μm pore size filter (NeuroProbe, Gaithersburg, MD, 106–8). HG1-2 was mixed with the recombinant mouse CXCL13 in the assay buffer of 1×Hank's Balanced Salt Solution, 0.5% BSA, and 10 mM HEPES and dispensed into the bottom wells of the chemotaxis assay plates. Chemotaxis was initiated by adding to the top of the filter the Ba/F3/mCXCR5 cells mixed with HG1-2 and the reaction was incubated at 37°C, 5% CO2 for one hr. Cells migrated into the bottom wells were quantified with CyQuant (Invitrogen, Grand Island, C7026). The plates were read at Ex485/Em538 on a SpectraMax Gemini plate reader. The numbers of migrated cells were calculated based on standard curves generated by adding Ba/F3/mCXCR5 cell directly to the bottom wells.

Radiolabeled [I^{125}] Study to Measure CXCL13 Turnover Rate

Male DBA mice (no fasting; $N=3$ per time point) were administered 2 mM potassium iodine (KI) water 3–4 days prior to dosing I^{125} -CXCL13. DBA mice were administered 4 μg of I^{125} -CXCL13 (0.5 mCi) as a single i.v. bolus dose into the tail vein and blood samples were collected either by cardiac puncture or retro-orbital bleeding at 5 min, 15 min, 30 min, 60 min, 90 min, 2 h, 3 h, 6 h, 24 h time points after IV administration. Blood was collected into plasma EDTA tubes containing Roche complete protease inhibitor. Plasma was processed by centrifugation (900*g*) for all time points. Total radioactivity and TCA-precipitable soluble counts in plasma sample were measured by gamma counting. SDS-PAGE indicated CXCL13 as intact protein in plasma samples (data not shown). TCA-precipitable radioactivity cpm was used for the PK calculations.

Mouse CXCL13 (BLC/BCA-1) (R&D systems, Minneapolis, MN, catalogue # 470-BC-025/CF Lot BPP0610081) was iodinated using Bolton-Hunter methods by Perkin Elmer, with 98% I^{125} incorporation (TCA precipitated counts). The I^{125} -CXCL13 had a specific activity of 2,200 Ci/mmol. *In vitro* assessment of labeled CXCL13 stability in plasma was completed prior to dosing (data not shown).

ELISA for HG1-2 Serum PK

Concentrations of free HG1-2 antibody in serum were determined by an enzyme-linked immunosorbent assay (ELISA) with a quantitative range of 25.6–3.37 ng/mL in 5% serum. Samples were diluted in a Tris High Salt Buffer containing 0.05% (v/v) Tween 20, 1% (w/v) BSA and 0.05% (v/v) Proclin™ 300 to the Minimum Required Dilution (MRD) of 1:20 followed by additional dilutions required in a Tris High Salt Buffer containing 0.05% (v/v) Tween 20, 1% (w/v) BSA and 0.05% (v/v) Proclin™ 300 and 5% Sprague–Dawley Rat serum. Recombinant mouse CXCL13/BLC/BCA-1 (Invitrogen/Gibco, Carlsbad California) was used at 1.0 μg/mL in Phosphate Buffered Saline (Calcium and Magnesium Free) and captured on Costar 3590 96-well High Bind EIA plates (Corning, Inc., Corning, NY) overnight at approximately 2–8°C and then blocked with Tris High Salt Buffer containing 0.05% (v/v) Tween 20, 1% (w/v) BSA and 0.05% (v/v) Proclin™ 300 after washing with Tris High Salt Buffer containing 0.05% Tween 20. The optical density reading was obtained at 450 nm on a Molecular Devices plate reader utilizing Softmax Pro 5.2 software. The anti-mCXCL13 standards were used to construct a standard curve using Watson LIMS (Laboratory Information Management System) version 7.4 and Logistic Auto Estimate curve fitting (Thermo Fisher Scientific, Waltham, MA). Serum concentrations of samples containing anti-mCXCL13 were extrapolated from this curve.

ELISA for Total CXCL13 Levels in Serum and Spleen

ELISA assay to measure total (free and antibody bound) CXCL13 was developed using polyclonal anti-CXCL13 antibodies as capture antibody (R&D Systems, Minneapolis, MN). 96 well ELISA plates were coated with capture antibody overnight at room temperature. The plates were washed with PBS-T (PBS + 0.05% Tween-20) and blocked with PBS + 1% BSA for 2 h at room temperature. Mouse serum samples or spleen extracts were diluted in PBS-T + 1% BSA and added

to the coated plates. The mixture was incubated at room temperature for two hours. The plates were then washed with PBS-T, followed by the addition of a biotinylated polyclonal anti-CXCL13 secondary antibody (R&D Systems, Minneapolis, MN) and incubated at room temperature for two hours. The plates were then washed again, and the bound secondary antibodies were detected with Poly-HRP Streptavidin (ThermoScientific, Waltham, MA) and TMB substrate (KPL, Gaithersburg, MD) according to the manufacturer's instructions. Absorbance at 450 nm was acquired on a Perkin Elmer Envision plate reader. CXCL13 levels were calculated with standard curves generated with recombinant CXCL13.

To prepare mouse spleen extracts, frozen mouse spleens were weighed and mixed with 1.0 mm Zirconium Oxide beads (Next Advance, Averill Park, NY) in ice cold PBS, 0.1% Igepal CA-630 (Sigma, I8896), 1% BSA and Protease Inhibitor cocktail (Sigma, St. Louis, MO). The spleens were then homogenized using a Bullet Blender (Next Advance, Averill Park, NY) for 10 min at 4°C. Supernatants were collected and used for ELISA analysis as above.

Data Analysis and Fitting

Estimation of Antibody Binding Affinity to Endogenous CXCL13

The equilibrium binding constant (Kd) for HG1-2 to the endogenous CXCL13 in the mouse serum was calculated using nonlinear fit of the total concentration of antibody (D_{tot}), total concentration of CXCL13 (R_{tot}) and corresponding free CXCL13 (R_{free}) from the assays described in section "Serum ELISA for Antibody Affinity to Endogenous CXCL13". The data was fitted to the Eq. 1 below describing the mathematical relationship between three sets of concentrations[13]. Phoenix WinNonLin software v6.1 (Pharsight Corporation, Cary, NC) was used to perform nonlinear fit.

$$R_{tot}-R_{free}=\frac{(Kd+D_{tot}+R_{tot})-\sqrt{(Kd+D_{tot}+R_{tot})^2-4*D_{tot}*R_{tot}}}{2} \quad (1)$$

Estimating CXCL13 Serum Turnover

The data obtained in serum using an i.v. dose of radiolabeled recombinant mCXCL13 were fitted using WinNonLin-Phoenix v6.1 (Pharsight Corporation, Cary, NC). Given the bi-exponential decay observed in the serum, a 2-compartmental pharmacokinetic model was applied and model parameters were estimated in order to calculate the serum turnover rate (Kdeg) and corresponding half-life of CXCL13. The default option of the Gauss-Newton (Levenberg and Hartley) algorithm was chosen to perform the minimization with 0.0001 as the convergence criterion. All available weighting options were applied to the data, and the model with the best fit was chosen based on the parameter precision and visual diagnostics.

Site-of-Action Model

Model of Antibody PK and Total CXCL13 Levels in Serum

MONOLIX v3.2 was used to perform all the data fitting and model estimation (14). A quasi-equilibrium approximation was applied that assumes that the free drug, target and the complex are in rapid equilibrium since the *in vivo* distribution and elimination process are typically slower compared to the on- and off-rates of antibody binding. The following set of equations describes the *in vivo* kinetics of drug, target, complex and the mathematical relationships between them:

$$\frac{dD_{tot}}{dt}=\frac{KA*Dip}{Vc\_F}-Kel*D_{free}-\frac{R_{tot}*K_{com}*D_{free}}{(KSS+D_{free})} \quad (2)$$

$$\frac{dR_{tot}}{dt}=K_{syn}-K_{deg}*R_{tot}-(K_{com}-K_{deg})*\frac{R_{tot}*D_{free}}{(KSS+D_{free})} \quad (3)$$

$$DR=R_{tot}*\frac{D_{free}}{(KSS+D_{free})} \quad (4)$$

$$R_{tot}-R_{free}=\frac{1}{2}\left[(D_{tot}+R_{tot}+KSS)-\sqrt{(D_{tot}+R_{tot}+KSS)^2-4*D_{tot}*R_{tot}}\right] \quad (5)$$

$$K_{syn}=Ro*K_{deg} \quad (6)$$

Equations 2 and 3 describe the kinetics of total drug levels ($Dtot$) and total CXCL13 levels ($Rtot$). Equations 4 and 5 mathematically describe free drug and complex levels as a function of total drug and target concentration. Equation 6 describes *in vivo* synthesis rate of CXCL13 ($Ksyn$) as a function of endogenous turnover rate ($Kdeg$) and the pre-treatment (i.e. baseline) levels of CXCL13 (Ro).

The turnover rate constants of free drug (D_{free}), free target (R_{free}) and complex (DR) are denoted as Kel, $Kdeg$ and $Kcom$ respectively. KA and Vc_F denote the absorption rate constant through the i.p. route, and the volume of distribution divided by the bioavailability. Dip is the drug amount at the i.p. dosing site. The binding affinity constant *in vivo* is denoted by KSS.

Equations 2–6 were used to fit the observed serum data from single dose studies and key model parameters were estimated.

Model of Total CXCL13 Levels in Spleen Tissue

The model for describing antibody and total CXCL13 levels in spleen was an extension of the serum model wherein the antibody distribution to the tissue and turnover kinetics of CXCL13 and complex half-life in spleen were taken into account in order to model the CXCL13 kinetics at the target tissue. The binding kinetics equations describing antibody and CXCL13 kinetics in spleen tissue are as follows:

$$D'_{free} = 0.3 * D_{free} \tag{7}$$

$$\frac{dRtot'}{dt} = Ksyn' - Kdeg' * Rtot' - (Kcom' - Kdeg') * \frac{Rtot' * D'_{free}}{\left(KSS + D'_{free}\right)} \tag{8}$$

$$DR' = Rtot' * \frac{D'_{free}}{\left(KSS + D'_{free}\right)} \tag{9}$$

$$R'_{tot} - R'_{free} = \frac{1}{2}\left[\left(D'_{tot} + R'_{tot} + KSS\right) - \sqrt{\left(D'_{tot} + R'_{tot} + KSS\right)^2 - 4 * D'_{tot} * R'_{tot}}\right] \tag{10}$$

$$Ksyn' = Ro' * Kdeg' \tag{11}$$

Equation 7 describes free antibody levels in spleen (D'_{free}) as a function of free antibody levels in serum (D_{free}). Equation 8 describes the kinetics of total CXCL13 levels (R'_{tot}) in spleen Eqs. 9 and 10 mathematically describe complex levels and free target in spleen as a function of total drug and target concentration in spleen. Equation 11 describes *in vivo* synthesis rate of CXCL13 ($Ksyn'$) as a function of endogenous turnover rate ($Kdeg'$) and the pre-treatment (i.e. baseline) levels of CXCL13 (Ro').

D_{free} is the free antibody levels in serum; D'_{free} and $Rtot'$ denote free drug and total CXCL13 in spleen; $Kcom'$ and $Kdeg'$ represent the spleen turnover rate constant of free (R') and bound CXCL13 (DR') respectively. Baseline (i.e. pre-treatment) levels of CXCL13 in spleen is denoted as Ro'.

Similar to the serum model, complex turnover rate (i.e. $Kcom'$) in spleen was assumed to be same as free antibody turnover rate (i.e. Kel). The values of apparent binding affinity constant (KSS) *in vivo* and Kel are estimated using serum model, thus the only key parameter to be estimated from spleen data is the spleen turnover rate of CXCL13 ($Kdeg'$).

Inhibitor Effect Sigmoidal Model for Target Coverage-PD Response Relationships

The relationship between target coverage (COV) in spleen and the resulting PD response (E) was modeled using following equation:

$$E = E0 * \left[1 - \frac{COV^{\gamma}}{(COV^{\gamma} + COV50^{\gamma})}\right] \tag{12}$$

Where, $E0$ is the baseline PD response pre-treatment, $COV50$ is the level of target coverage that results in 50% suppression of PD response over baseline, and γ is the hill coefficient to account for the steepness of response.

RESULTS

In Vitro Potency of HG1-2 Antibody

The potency of the murine CXCL13 neutralizing antibody HG1-2 was assessed *in vitro* to confirm its suitability for *in vivo* dosing in mouse studies. Antibody affinity was measured using both recombinant and endogenous CXCL13 present in mouse serum. Using BIAcore, the equilibrium binding constant (K_d) of the antibody to the recombinant mCXCL13 was estimated to be 0.04 nM, with a k_{on} value of 2.1×10^6 $M^{-1}S^{-1}$ and k_{off} of 8.1×10^{-5} S^{-1} (Table II). The affinity of HG1-2 for the endogenous CXCL13 in mouse serum was evaluated using ELISA assay measuring free CXCL13 in the presence of varying concentrations of the antibody. The equilibrium binding constant of HG1-2 for endogenous CXCL13 was estimated to be 2.2 nM (Table II). As an additional measure of antibody potency in a functional assay, neutralizing activity of HG1-2 was assessed in transwell chemotaxis assay with mouse pre-B cell line Ba/F3 overexpressing the CXCL13 receptor CXCR5. The IC_{50} of the HG1-2 for neutralizing mCXCL13 in this assay was determined to be 1.3 nM (Table II).

The wide difference (~50 fold) between BIAcore- and ELISA-based affinities may reflect the nature of antibody binding to recombinant *vs*. endogenous protein, as well as solid phase *vs*. native solution phase conditions. Varying results from the measurements described above indicate that the *in vitro* determination of HG1-2 affinity depended upon the

Table II *In Vitro* Potency of HG1-2 in Different Assays

Antibody	BIAcore			Serum ELISA	Chemotaxis assay
	K_{on} 1E+06 (M^{-1} s^{-1})	K_{off} 1E-05 (s^{-1})	K_d [a] (nM)	K_d [b] (nM)	IC50 (nM)
HG1-2	2.1 ± 0.3	8.1 ± 1.3	0.04[a]	2.2[b]	1.3 ± 0.4

K_{on} is the association binding constant and K_{off} is the dissociation binding constant

[a] Equilibrium binding affinity constant (K_d) for recombinant CXCL13, derived using $K_d = K_{off} / K_{on}$

[b] Equilibrium binding affinity constant (K_d) for endogenous CXCL13

experimental conditions, and warranted further characterization of potency in *in vivo* conditions.

In Vivo Activity of HG1-2 Antibody

In vivo target modulation and pharmacological activity of HG1-2 was studied in a mouse T-dependent immunization (TDI) model immunized with hapten carrier conjugate nitrophenyl:chicken gamma globulin (NP-CGG). We utilized TDI model as an initial surrogate for antibody driven autoimmunity as this model has a high level of reproducibility and defined onset that work well for PK/PD model development.

Table I provides details of *in vivo* study design and dose levels. First, a single-dose PK/PD study was conducted in the TDI mice with a 10 mg/kg i.p. dose of HG1-2. In this study, a full time course of antibody levels in serum, and total CXCL13 in both serum/spleen were obtained up to 168 h post-dose. Secondly, a multiple-dose study was conducted using immunized mice randomized in separate groups, and dosed with IgG control, and 3, 10 and 30 mg/kg of HG1-2 given 3 times within 10-day period. In this study, impact of antibody treatment on the B cell follicle architecture and germinal centers was assessed. At the termination of the study, spleens were harvested and analyzed by immunohistochemistry for B cell follicles and germinal center response. Since the primary focus of 10-day multiple-dose study was to explore germinal center response, only limited plasma samples were available to study antibody exposures and modulation of CXCL13 levels.

Following sections describe development of SoA model using PK/PD data from single dose study, application of the model to estimate target coverage in multiple-dose study, and correlation of target coverage to PD response (i.e. #GC/mm^2).

Site-of-Action Model Development

Antibody exposures and total CXCL13 levels (i.e. free and complex) post dosing were analyzed using a novel binding-kinetics model that takes into account the antibody binding and *in vivo* turnover rates of antibody, free CXCL13 and the drug-target complex in both serum and site-of-action (i.e. spleen) (Fig. 1). Antibody distribution into the tissue and subsequent modulation of the target at the target site of action is also taken into account in the model. This modeling framework, referred as site-of-action (SoA) model henceforth, is an extension of target-mediated drug disposition models originally described by Mager and co-workers, and recently investigated by others (15–18).

The SoA modeling analysis was performed in a sequential manner in which serum and spleen data from single-dose study were fitted first to estimate key model parameters (Fig. 1). Subsequently, the model was applied to the multiple-dose study in which model was trained to account for differences in CXCL13 baseline levels and antibody PK when compared to single-dose study. The SoA model with estimated parameters was then utilized to quantify the target coverage in multiple dose study. Finally, the estimated target coverage was correlated to the PD (i.e.

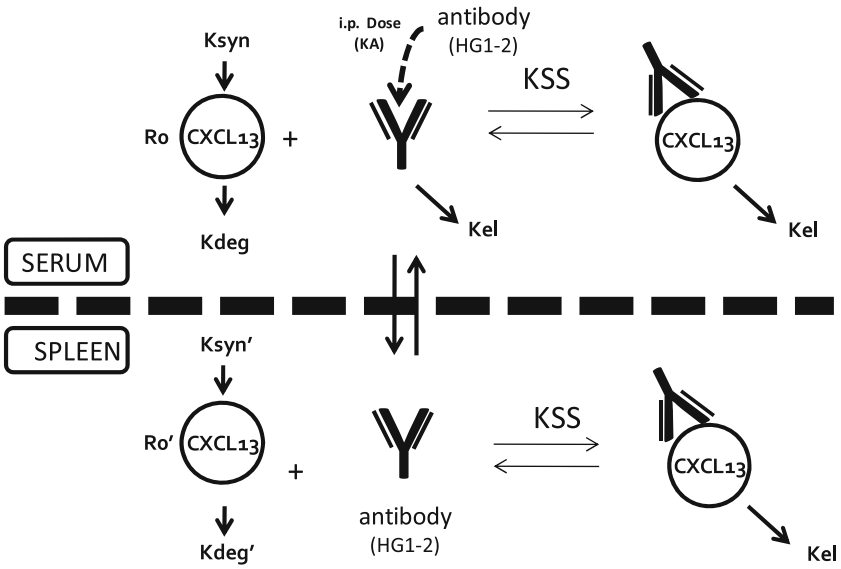

Fig. 1 Schematic of site-of-action (SoA) model. The SoA describes binding kinetics of HG1-2 antibody to CXCL13 in serum and target tissue (i.e. spleen). Target turnover rate in serum and spleen is denoted by Kdeg and Kdeg′, respectively. Baseline (i.e. pretreatment) levels of CXCL13 in serum (Ro) and spleen (Ro′) are also taken into account by the model. KSS is the *in vivo* binding equilibrium binding constant of antibody-target interactions. Antibody pharmacokinetics are described by the turnover rate constant (Kel), central volume of distribution (Vc_F) and the absorption rate constant (KA) through i.p. route.

GC response) towards building target coverage-PD response relationships.

To aid in the model development, a key parameter in the model, i.e. CXCL13 turnover rate in serum (Kdeg) was experimentally measured using a radiolabeled study in mouse. Also, complex eliminate rate (i.e. *Kcom*) was assumed to be same as free antibody turnover rate (i.e. *Kel*). The K_{deg} parameter was estimated to be 0.94 h^{-1} and corresponding half-life was 44 min (Supplementary Material). The estimated half-life is consistent with the fact that the molecular weight of CXCL13 (~10 kDa) is within the cut-off limits of renal clearance (<60 kDa). For cytokines and chemokines within this cut-off range, the typical half life is <1 h (19,20).

Modeling of Total CXCL13 Levels in Serum After Single Dose

Post antibody treatment, the total serum CXCL13 levels increased ~15 fold from a mean baseline of 221pM to ~3000pM. The increase in total target level is due to the stabilization of circulating CXCL13 in complex with the antibody. This is a commonly observed phenomenon in the case of antibodies against soluble targets (21,22) whereby the equilibrium is shifted from free target (turning over with a faster rate) to the antibody-bound target (turning over at a slower rate) resulting in decreased free levels in spite of the increased total target levels (i.e. free + complex).

Total CXCL13 levels (i.e. free and complexed with HG1-2) observed in serum upon antibody dosing were fitted using the SoA model to estimate key model parameters. Figure 2a and b present the observed *vs*. model fits of the serum data. The model described the antibody pharmacokinetics and resulting increase in total CXCL13 reasonably well given the intrinsic variability in the data obtained from different animals. The mean baseline chemokine levels (R_o) in serum prior to the antibody dosing was fixed to the observed mean of 221pM, and Kdeg was fixed to experimentally estimated value of 0.94 h^{-1}. Table III summarizes the estimated model parameters for the serum compartment. The serum turnover rate of antibody (Kel) was estimated to be 0.012 (1/h) corresponding to a half life of 58 h. The *in vivo* binding affinity constant (KSS) was estimated to be 16.7 nM. This estimated *in vivo* affinity differs significantly from the Kd value assessed using BIAcore (0.04 nM *vs*. 16.7 nM) but in the range of affinity value (2.2 nM) obtained for the endogenous CXCL13 in mouse serum. This is not surprising given that assay conditions of *in vitro* BIAcore setup can vary considerably from the *in vivo* physiological conditions in terms of recombinant *vs*. endogenous target, *in vitro* solid phase *vs*. *in vivo* solution, and the presence of CXCL13 receptor binding *in vivo*. Disconnect between *in vitro vs*. *in vivo* affinity has previously been noted for

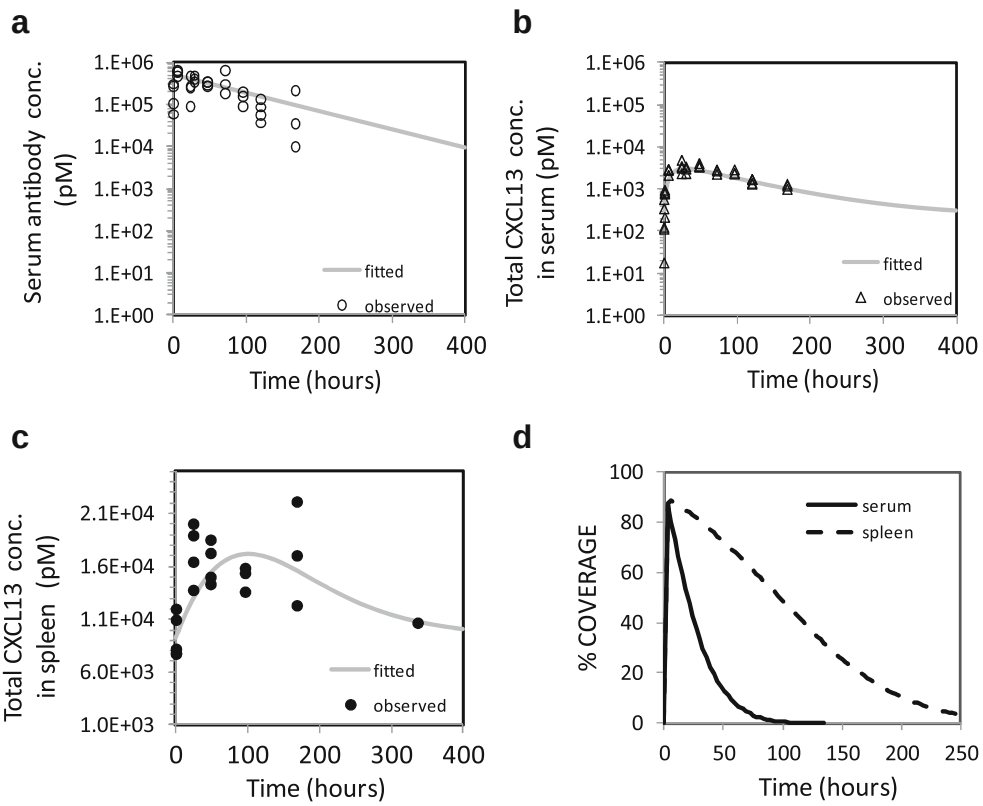

Fig. 2 Site-of-action model fitting of single-dose PK/PD study with 10 mg/kg of HG1-2. (**a**) HG1-2 antibody levels in serum, observed (*open circles*) *vs*. fitted (*solid line*). (**b**) Total CXCL13 levels in serum, observed (*open triangles*) *vs*. fitted (*solid line*). (**c**) Total CXCL13 levels in spleen, observed (*open squares*) *vs*. fitted (*solid line*). (**d**) Simulated % target coverage in serum (*solid line*) and spleen (*dotted line*).

various antibodies including anti-CD4 in human (0.6 nM *in vitro vs*. 19.38 nM *in vivo*) (23). Ultimately, it's the *in vivo* estimated affinity that is the most relevant potency parameter driving target modulation in animals.

Modeling of Total CXCL13 Levels in Spleen After Single Dose

The change in CXCL13 total level in spleen post-dose was only modest - an increase of 2–3 fold over the baseline of 9303 pM (Fig. 2c). Each of the data points in Fig. 2c represents a terminal spleen sample from an individual animal, and high variability in total CXCL13 is seen between the animals. Even with the inherent variability among individual animals, the model gives a reasonable description of the overall trend for the total spleen CXCL13. Table III summarizes the model parameters relevant to the spleen tissue. The mean baseline level ($R_o^{'}$) in spleen was fixed to the observed mean of 9303 pM. Similarly, KSS and Kel parameters were fixed to the values estimated from serum data (Table III). Thus, the turnover rate ($K_{deg}^{'}$) of CXCL13 in spleen was the key parameter to be estimated using spleen data. This $K_{deg}^{'}$ parameter represents both the consumption of CXCL13 within spleen and the distributive clearance rate from spleen to serum. The $K_{deg}^{'}$ parameter was estimated to be 0.027 (1/h) which corresponds to a half life of 25 h. This estimated value is consistent with the >2 fold increase seen in total CXCL13 levels in spleen. Upon antibody binding, the complex adopts the antibody half-life resulting in stabilization of free CXCL13 in spleen from a half life of 25 h for free spleen CXCL13 to 58 h for antibody complex (>2-fold difference).

Modeling of Total CXCL13 Levels in Serum After Multiple Doses

In the multiple dose study, serum levels of HG1-2 and total CXCL13 in all three dose groups were measured at three specific time points: 6 h after the first dose, 24 h and 72 after the third dose. Similar to the 10 mg/kg single dose study, the total CXCL13 levels in the serum increased after dosing, with 30 mg/kg dose group showing highest total CXCL13 levels (Fig. 3). Mean concentrations of total CXCL13 after 3rd dose were higher than those at 6 h time point after the first dose, indicating the accumulation of bound CXCL13 upon subsequent dosing.

The pharmacokinetic and total CXCL13 data were fitted by the SoA model to take into account study-specific CXCL13 baseline levels and antibody PK observed in the multiple-dose study. The target-specific parameters (e.g. free CXCL13 half-life of 44 mins, and K_d value of 16.7 nM were kept fixed to the values determined by the single 10 mg/kg dose study, since these parameters are intrinsic to the properties of endogenous CXCL13 and the antibody, and independent on the study type and PK variation. The estimated baseline CXCL13 levels for three dose levels were in the range of 117–264 pM, but slightly different from the baseline mean of 221pM from single-dose study. As Fig. 3 shows, the model described the total CXCL13 levels well based on the fitted *vs*. observed data, providing confidence in the validity of target-specific parameters estimated from the 10 mg/kg single dose study.

In Vivo Target Coverage Post HG1-2 Treatment

Having estimated the key model parameters using the single- and multiple-dose data, the SoA model was utilized to estimate unbound (i.e. free) CXCL13 levels in serum and tissue. The free CXCL13 levels post dosing, normalized to the baseline level pretreatment provide a measure of % target coverage defined as (1 – free CXCL13/baseline)*100.

Target Coverage in Serum and Spleen After Single Dose

Figure 2d presents the time profile of % target coverage after 10 mg/kg single dose. As depicted, peak coverage in serum and spleen is similar (i.e. 90%) but the serum profile returns to the 0%

Table III Estimates of Site-of-Action Model Parameters

Parameter	Definition	Units	Estimate (%RSE) Plasma	Estimate (%RSE) Spleen
KA	Absorption rate constant	(1/h)	0.607 (11%)	–
Vc_F	Central volume of distribution of antibody divided by the bioavailability (F)	(L/kg)	0.136 (19%)	–
Kel	Serum turnover rate of antibody	(1/h)	0.012 (14%)	0.012 (FIX)
Kdeg & Kdeg′	Turnover rate constant of CXCL13 in serum and spleen	(1/h)	0.94 (FIX)	0.027 (26%)
Ro & Ro′	Baseline levels of CXCL13 in serum and spleen	(pM)	221 (FIX)	9303 (FIX)
KSS	*In vivo* binding affinity of antibody	(nM)	16.7 (15%)	16.7 (FIX)

Serum antibody levels along with the total CXCL13 levels in serum and spleen from single-dose TDI study were utilized to obtain key model parameters. Model parameters with observed mean values or estimated using experiments were fixed during model fitting

% *RSE* %root square error

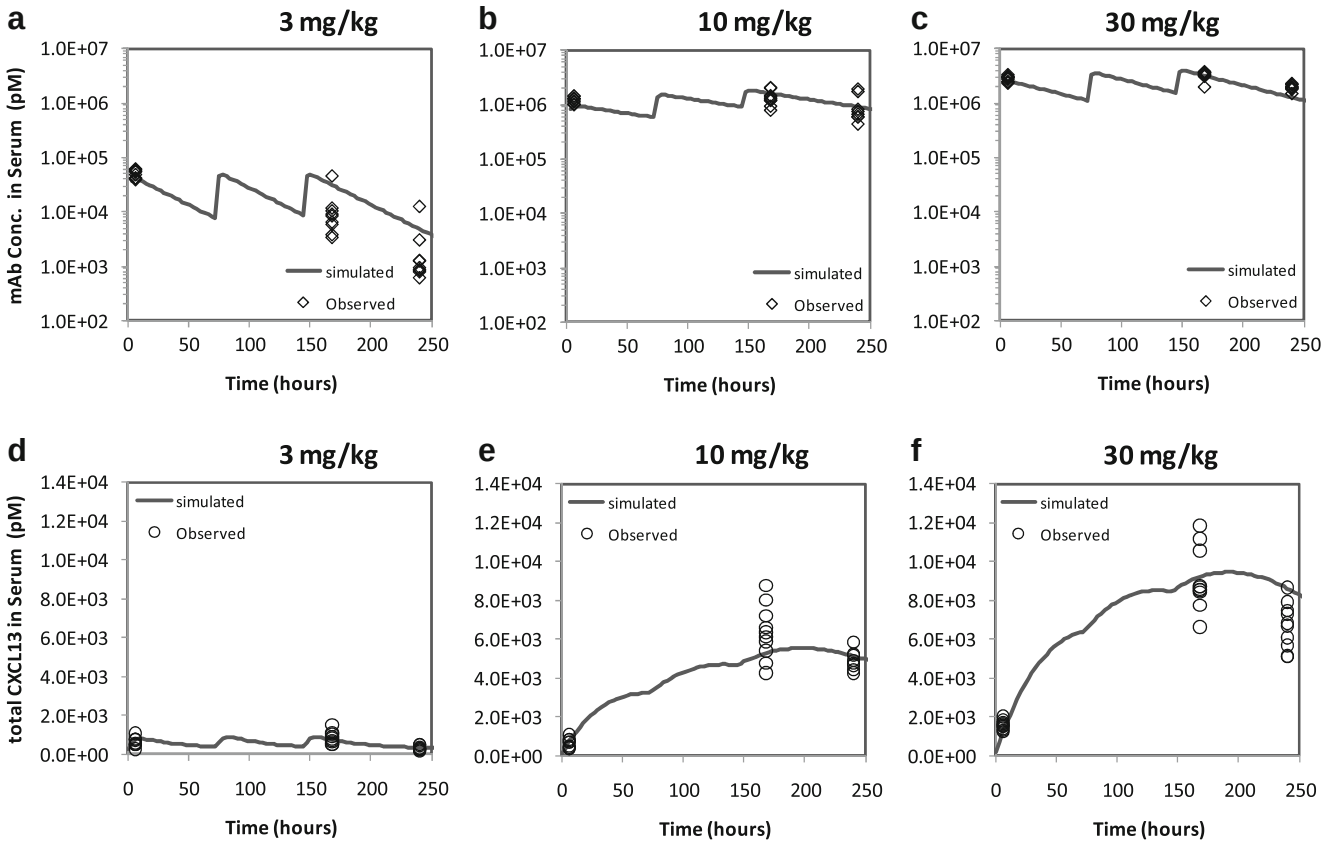

Fig. 3 Site-of-action model fitting of PK/PD data obtained from multiple-dose TDI studies. (**a**, **b**, **c**) HG1-2 levels in serum at 3, 10 and 30 mg/kg, respectively, fitted (*solid line*) *vs*. observed (*open diamonds*). (**d**, **e**, **f**) Total CXCL13 levels in serum, at 3, 10 and 30 mg/kg respectively, fitted (*solid line*) *vs*. observed (*open circles*).

target coverage within 100 h. In contrast, the spleen coverage is sustained at 50% at 100 h. Hence, a relatively greater level of target suppression is reached in tissue compared to the serum. This result is a consequence of a slow turnover rate of CXCL13 in tissues (half life of 25 h) *vs*. faster serum turnover (half life of 44 mins). This implies that the magnitude of target accumulation in spleen is lower (2–3×) compared to serum (15×). Thus, as a consequence of binding kinetics, HG1-2 is able to achieve higher target coverage in spleen compared to serum at the same dose level.

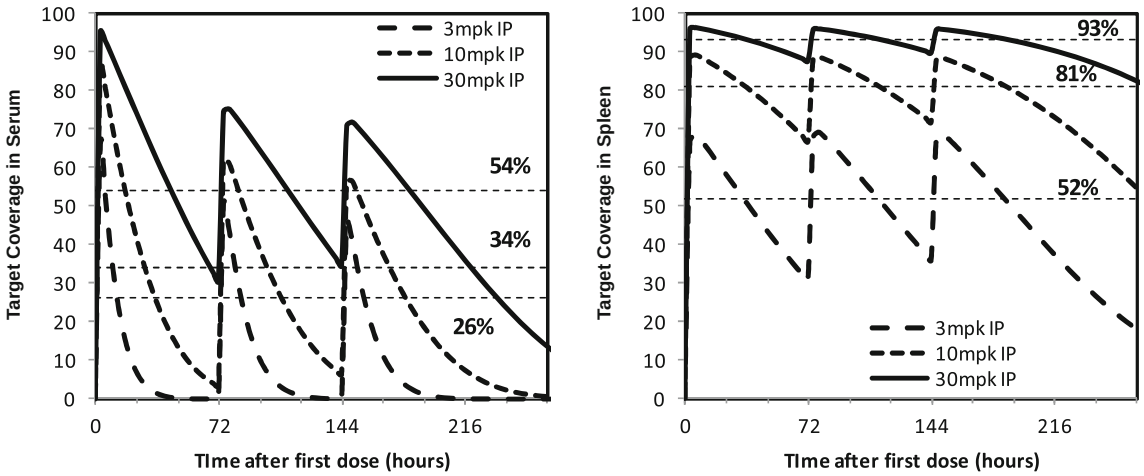

Fig. 4 Projected level of CXCL13 target coverage in serum (**a**) and spleen (**b**) at 3, 10 and 30 mg/kg dose in multiple-dose TDI study. *Horizontal dotted lines* represent the time averaged target coverage (i.e. CXCL13 suppression) projected by the site-of-action model at 3, 10 and 30 mg/kg.

Target Coverage in Serum and Spleen After Multiple Doses

The SoA trained on the multiple dose data was used to project the target coverage in serum (Fig. 4a) and spleen (Fig. 4b) at 3, 10 and 30 mg/kg. Similar to the single dose study, % target coverage level (averaged over dosing period) in the spleen was projected to be higher than in the serum at the same dose level. For example, the 10 mg/kg dose group produced an average coverage of 81% in spleen (Fig. 4b) whereas only 34% average coverage was seen in serum (Fig. 4a). In spleen, higher target coverage was seen with increasing doses. For example, 30 mg/kg dose produced an average of 93% target coverage in spleen, whereas 3 mg/kg dose produced only 52% target suppression in spleen (Fig. 4b).

Correlation Between Germinal Center Response and Target Coverage

As shown in Fig. 5, HG1-2 treatment disrupted the architecture of splenic B cell follicles in a dose-dependent manner. The B cell follicles present in spleens obtained from mice treated with 10 and 30 mg/kg of HG1-2 adopted a ring- like configuration around the peri-arteriolar lymphoid sheath and lacked clearly defined interfollicular regions (Fig. 5, panels for 10 and 30 mpk). In contrast, B cell follicles present in the 3 mg/kg treated group appeared similar to follicles observed in control antibody-treated animals, which were well-defined and separated by interfollicular regions (Fig. 5, panel for 3 mg/kg). Anti-CXCL13 treatment also affected the physical location of germinal centers relative to the B cell follicles. Mice treated with 10 or 30 mg/kg of HG1-2 developed germinal centers outside the B cell follicles and adjacent to the periarteriolar lymphatic sheath (PALS). By contrast, mice treated with control antibody or 3 mg/kg of HG1-2 developed large well-defined germinal centers that were embedded in B cell follicles.

Impact of HG1-2 on the germinal center response was quantified in terms of number of GC per square area (GC/mm^2) and correlated with spleen target coverage in order to explore target coverage-PD relationships (Fig. 6a, b). A Sigmoidal inhibitory effect model was utilized to fit the target coverage-PD response data to estimate the target coverage that results in 50% suppression of PD response. The model fit is depicted in Fig. 6b by

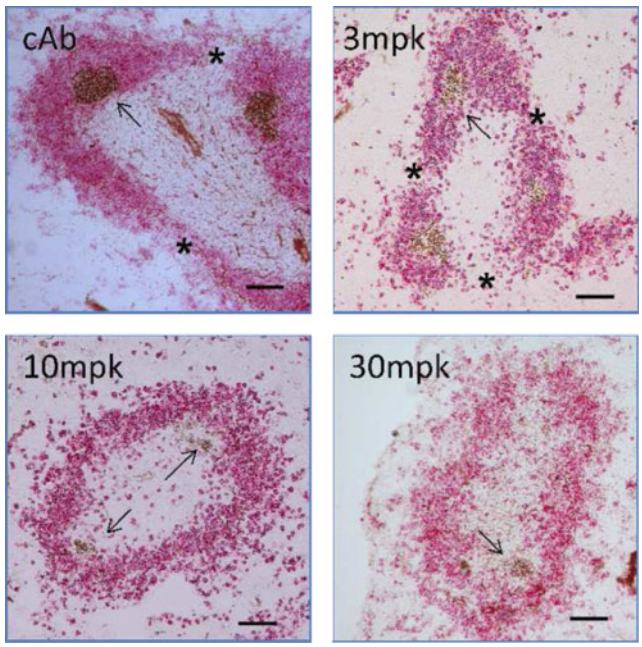

Fig. 5 Impact of anti-CXCL13 antibody treatment on B cell follicle structure and germinal center characteristics. Photomicrographs show IgD (*red*) and PNA (*brown*) stained spleen sections obtained from mice treated with control (cAb) or anti-CXCL13 (3, 10, 30 mg/kg) antibody. Scale bar indicates 100 mm. *Arrows* highlight PNA+ germinal centers and *stars mark* interfollicular regions.

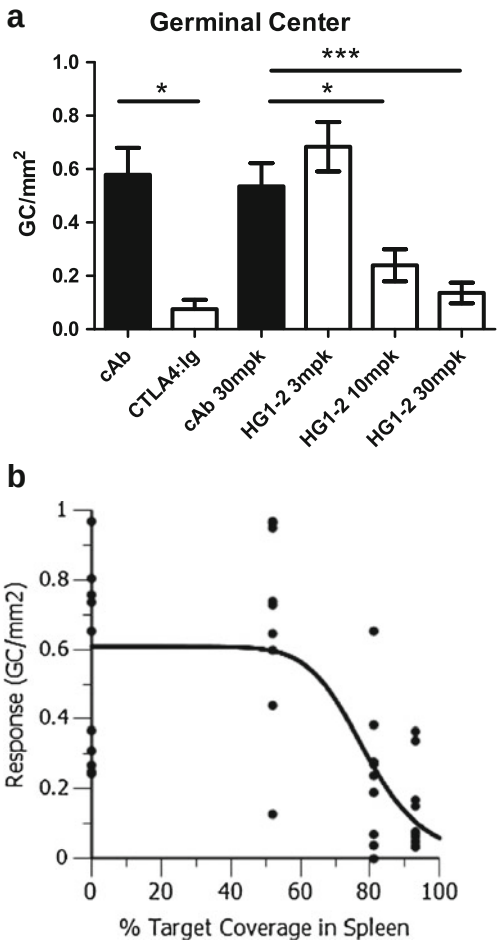

Fig. 6 Impact of Anti-CXCL13 antibody treatment on germinal center numbers. (**a**) Number of germinal centers per unit area (GC/mm^2) of spleen measured for control (cAb), positive control (CTLA4 Ig), 3, 10, 30 mg/kg HG1-2 dose groups. *Bars* represent the average for the treatment groups and *error bars* indicate SEM. *$p \leq 0.03$; **$p = 0.091$; ***$p \leq 0.0007$; Mann–Whitney U-test. (**b**) Spleen target coverage *vs*. PD response fitted by a Sigmoidal inhibitory effect model. Observed data shown in *solid circles*, and model fit with *solid line*.

solid line along with the observed data (solid circles). The mean baseline response (E0) was estimated to be 0.61 GC/mm^2 (9% coefficient of variation (CV)) and target coverage for 50% suppression, COV50, was estimated to be 79% (7% CV). The Hill coefficient (γ) was estimated to be 9.4 but this value was not estimated precisely as indicated by a CV of 70%. As shown in Fig. 6a, HG1-2 doses above 3 mg/kg resulted in statistical significant response over controls with 30 mg/kg dose producing the largest effect. When the PD response is plotted as a function of %target coverage achieved (Fig. 6b), a steep non-linear relationship can be seen within 3–30 mg/kg dose range. For target coverage <50%, no meaningful impact on germinal centers is seen. For target coverage > 50%, higher target coverage results in greater PD suppression. At 30 mg/kg with 93% spleen target coverage, pharmacological response is close to the maximum.

DISCUSSION

This study illustrates the *in vivo* pharmacological role of CXCL13 using an anti-mouse CXCL13 antibody. A thorough quantitative analysis of PK and PD endpoints in single- and multiple-dose TDI studies was performed in order to establish the dynamic link between serum antibody exposures and total CXCL13 levels in serum and spleen. The results from our studies demonstrated that CXCL13 inhibition altered structure of B cell follicles in the spleen in a dose-dependent fashion, with similar phenotype as revealed by immunohistochemistry staining of spleen section as the CXCL13 and the CXCR5 knockout mice (1). We observed reduced number and size of germinal centers in the spleen during a T dependent antigen induced immune response, and the germinal centers that did form were dislocated outside of the B cell follicles. This is again consistent with what was seen in the CXCL13 and CXCR5 knockout animals (1). However, this is a unique study demonstrating disruption of spleen B cell follicle architecture in mature adult animals post developmental stage by pharmacological inhibition of CXCL13, indicating that the maintenance of homeostatic secondary lymphoid tissue structure is a dynamic process post organ development, and highlighting the prominent role of CXCL13 in this process. Therefore, long term CXCL13 inhibition could conceivably affect multiple biological responses as a result of compromising the integrity of B cell follicles in secondary lymphoid tissues.

In order to integrate available PK/PD data towards building exposure-response relationships, we developed a quantitative SoA model that was used to estimate the degree of CXCL13 coverage as a function of antibody dose. The SoA model is an extension of target-mediated drug disposition models (15–18) and describes antibody target binding kinetics in both serum and relevant target tissue. In the past, such models have generally been used to describe the serum kinetics of antibodies and proteins exhibiting non-linear behavior (24–27). More recently, these models have been used to integrate both the drug exposures and free and/or total target levels in serum (21,22,28). In none of these cases, tissue levels of target were available and to our knowledge this report provides the first example of a study where both the serum and tissue target levels were utilized to develop target-coverage-PD relationships at the site of action.

The relationship between antibody, target and complex is highly nonlinear in nature, and adequate experimental data need to be supplied to avoid the over-parameterization of the SoA model. *In vivo* turnover rates of free CXCL13 and complex (*Kdeg* and *Kcom* respectively) are two of the key parameters dictating degree of target coverage upon antibody dosing. To facilitate robust model development, a radiolabeled study was performed to estimate the *in vivo* turnover rate of CXCL13 (i.e. *Kdeg*). Further, a reasonable approximation was made for the complex turnover rate (i.e. *Kcom*) and it was assumed to be the same as the free antibody turnover rate (i.e. *Kel*). This is reasonable for small soluble targets such as CXCL13 (molecular weight ~ 10 kDa), since the molecular weight of complex is roughly equal to that of the free antibody and catabolic degradation of complex is likely to be similar to that of the free drug, as seen in the case of VEGF ligand in complex with bevacizumab (29). With the experimentally determined value of *Kdeg*, and the approximation for the *Kcom*, the number of model parameters to be estimated is reduced by two, greatly enhancing the model stability and precision of remaining parameters to be estimated. Since the antibody levels in spleen were not available in our studies, learnings from published radiolabeled studies of antibodies were utilized to facilitate the mechanistic analysis (30). Tissue data across a range of such studies indicate that the steady state antibody levels in mouse spleen interstitium are ~30% of those in serum. Thus, antibody levels in the spleen tissue of TDI animals are assumed to be 30% of serum levels.

With the estimated value of 16.7 nM for *in vivo* binding constant (KSS), the SoA model allowed the projection of unbound (i.e. free) CXCL13 levels and corresponding target coverage in serum and spleen. Free target levels post treatment and corresponding target coverage are technically challenging to measure experimentally (31,32), thus use of SoA models to predict target coverage in tissue from total levels is highly beneficial in drug development. Projections from SoA modeling indicate that in both single and multiple dose TDI studies, a relatively greater level of target suppression is achieved in spleen for a longer duration compared to the serum. For example, in multiple-dose TDI study, an average of 81% and 93% target suppression over dosing interval was achieved in spleen at 10 and 30 mg/kg respectively. In contrast, an average of only 34% and 54% target suppression was achieved in serum at these dose levels. In spite of low target suppression in serum at 10 and 30 mg/kg, antibody treatment

produced significant impact on the germinal center architecture, size and frequency (Figs. 5 and 6) due to the high level of target coverage (>80%) in spleen. At 3 mg/kg dose, target suppression in spleen was estimated to be 52%, a level at which no significant pharmacodynamic effects were seen when compared to the control arm, highlighting a steep relationship between target coverage and PD response. Indeed, the correlation analysis of target-coverage PD response shows that ~79% target coverage is required to achieve 50% PD suppression (Fig. 6b). Moreover, the maximum PD suppression in this study was seen at 30 mg/kg dose with 93% target coverage. Thus, to achieve effective blockade of CXCL13 pharmacology in human disease, a high tissue target coverage (>=93%) is likely to be required. In terms of free CXCL13, 93% target coverage implies ~650 pM of free CXCL13 (7% of pretreatment spleen CXCL13 levels, i.e. 9303 pM). It is the normalization of CXCL13 in the *target tissue* from the elevated disease levels to lower healthy levels that is likely to be the key for therapeutic benefit.

CONCLUSIONS

This work highlights the application of a unique SoA modeling analysis that integrates total target levels in circulation as well as in spleen to determine the target coverage at the tissue level. Results from the SoA modeling offer several insights towards rational development for anti-CXCL13 therapeutics in human. First, clinical doses of an anti-CXCL13 antibody or small molecule inhibitor should be designed to achieve a high degree of target coverage (>90%) in disease tissues towards neutralizing the CXCL13 function effectively. Secondly, the total target levels in serum and tissues can be used as an important biomarker of target engagement for a therapeutic under consideration. Thus, preclinical data package for a novel biotherapeutic (e.g. antibodies or fusion proteins) should involve exploration of dynamic relationship between drug exposures and total target levels in relevant disease tissues. This recommendation is valid not only for anti-CXCL13 biologics but also for antibodies against other soluble targets in serum or tissues. Such an exposure-response analysis will allow the estimation of *in-vivo* potency of the drug, and aid in the human dose projections. In conclusion, the quantitative relationships between target coverage and GC response described in this report pave the way for rational development of anti-CXCL13 therapeutics in disease indications where germinal center response and downstream pathways play an important role in underlying pathology.

ACKNOWLEDGMENTS AND DISCLOSURES

Authors wish to thank Quintus Medley, Ph.D. and Jill Wright, Ph.D. for reviewing the manuscript and proving useful suggestions.

This study was supported by Pfizer, Inc. All authors were employees of Pfizer at the time of study.

REFERENCES

1. Ansel KM, Ngo VN, Hyman PL, Luther SA, Forster R, Sedgwick JD, *et al*. A chemokine-driven positive feedback loop organizes lymphoid follicles. Nature. 2000;406(6793):309–14.
2. Cyster JG, Ansel KM, Reif K, Ekland EH, Hyman PL, Tang HL, *et al*. Follicular stromal cells and lymphocyte homing to follicles. Immunol Rev. 2000;176:181–93.
3. Legler DF, Loetscher M, Roos RS, Clark-Lewis I, Baggiolini M, Moser B. B cell-attracting chemokine 1, a human CXC chemokine expressed in lymphoid tissues, selectively attracts B lymphocytes via BLR1/CXCR5. J Exp Med. 1998;187(4):655–60.
4. Schaerli P, Willimann K, Lang AB, Lipp M, Loetscher P, Moser B. CXC chemokine receptor 5 expression defines follicular homing T cells with B cell helper function. J Exp Med. 2000;192(11):1553–62.
5. Amft N, Curnow SJ, Scheel-Toellner D, Devadas A, Oates J, Crocker J, *et al*. Ectopic expression of the B cell-attracting chemokine BCA-1 (CXCL13) on endothelial cells and within lymphoid follicles contributes to the establishment of germinal center-like structures in Sjogren's syndrome. Arthritis Rheum. 2001;44(11):2633–41.
6. Krumbholz M, Theil D, Cepok S, Hemmer B, Kivisakk P, Ransohoff RM, *et al*. Chemokines in multiple sclerosis: CXCL12 and CXCL13 up-regulation is differentially linked to CNS immune cell recruitment. Brain J Neurol. 2006;129(Pt 1):200–11.
7. Rosengren S, Wei N, Kalunian KC, Kavanaugh A, Boyle DL. CXCL13: a novel biomarker of B-cell return following rituximab treatment and synovitis in patients with rheumatoid arthritis. Rheumatology (Oxford, England). 2011;50(3):603–10.
8. Steinmetz OM, Velden J, Kneissler U, Marx M, Klein A, Helmchen U, *et al*. Analysis and classification of B-cell infiltrates in lupus and ANCA-associated nephritis. Kidney Int. 2008;74(4):448–57.
9. Serafini B, Rosicarelli B, Magliozzi R, Stigliano E, Aloisi F. Detection of ectopic B-cell follicles with germinal centers in the meninges of patients with secondary progressive multiple sclerosis. Brain Pathol (Zurich, Switzerland). 2004;14(2):164–74.
10. Shi K, Hayashida K, Kaneko M, Hashimoto J, Tomita T, Lipsky PE, *et al*. Lymphoid chemokine B cell-attracting chemokine-1 (CXCL13) is expressed in germinal center of ectopic lymphoid follicles within the synovium of chronic arthritis patients. J Immunol (Baltimore, Md : 1950). 2001;166(1):650–5.
11. Lee HT, Shiao YM, Wu TH, Chen WS, Hsu YH, Tsai SF, *et al*. Serum BLC/CXCL13 concentrations and renal expression of CXCL13/CXCR5 in patients with systemic lupus erythematosus and lupus nephritis. J Rheumatol. 2010;37(1):45–52.
12. Finch DK, Ettinger R, Karnell JL, Herbst R, Sleeman MA. Effects of CXCL13 inhibition on lymphoid follicles in models of autoimmune disease. Eur J Clin Investig. 2013;43(5):501–9.
13. Kamens JS. InventorCXCL13 binding proteins. USA patent US 2008/0227704 A1. 2008.
14. Chan PL, Jacqmin P, Lavielle M, McFadyen L, Weatherley B. The use of the SAEM algorithm in MONOLIX software for estimation of population pharmacokinetic-pharmacodynamic-viral dynamics parameters of maraviroc in asymptomatic HIV subjects. J Pharmacokinet Pharmacodyn. 2011;38(1):41–61.
15. Gibiansky L, Gibiansky E. Target-mediated drug disposition model for drugs that bind to more than one target. J Pharmacokinet Pharmacodyn. 2010;37(4):323–46.
16. Gibiansky L, Gibiansky E, Kakkar T, Ma P. Approximations of the target-mediated drug disposition model and identifiability of model parameters. J Pharmacokinet Pharmacodyn. 2008;35(5):573–91.

17. Mager DE. Target-mediated drug disposition and dynamics. Biochem Pharmacol. 2006;72(1):1–10.
18. Mager DE, Krzyzanski W. Quasi-equilibrium pharmacokinetic model for drugs exhibiting target-mediated drug disposition. Pharm Res. 2005;22(10):1589–96.
19. Bocci V. Interleukins. Clinical pharmacokinetics and practical implications. Clin Pharmacokinet. 1991;21(4):274–84.
20. Blick M, Sherwin SA, Rosenblum M, Gutterman J. Phase I study of recombinant tumor necrosis factor in cancer patients. Cancer Res. 1987;47(11):2986–9.
21. Gibiansky L, Frey N. Linking interleukin-6 receptor blockade with tocilizumab and its hematological effects using a modeling approach. J Pharmacokinet Pharmacodyn. 2012;39(1):5–16.
22. Lowe PJ, Renard D. Omalizumab decreases IgE production in patients with allergic (IgE-mediated) asthma; PKPD analysis of a biomarker, total IgE. Br J Clin Pharmacol. 2011;72(2):306–20.
23. Ng CM, Stefanich E, Anand BS, Fielder PJ, Vaickus L. Pharmacokinetics/pharmacodynamics of nondepleting anti-CD4 monoclonal antibody (TRX1) in healthy human volunteers. Pharm Res. 2006;23(1):95–103.
24. Betts AM, Clark TH, Yang J, Treadway JL, Li M, Giovanelli MA, *et al*. The application of target information and preclinical pharmacokinetic/pharmacodynamic modeling in predicting clinical doses of a Dickkopf-1 antibody for osteoporosis. J Pharmacol Exp Ther. 2010;333(1):2–13.
25. Luu KT, Bergqvist S, Chen E, Hu-Lowe D, Kraynov E. A model-based approach to predicting the human pharmacokinetics of a monoclonal antibody exhibiting target-mediated drug disposition. J Pharmacol Exp Ther. 2012;341(3):702–8.
26. Vugmeyster Y, Rohde C, Perreault M, Gimeno RE, Singh P. Agonistic TAM-163 antibody targeting Tyrosine kinase receptor-B: applying mechanistic modeling to enable preclinical to clinical translation and guide clinical trial design. mAbs. 2013;5(3):373–83.
27. Wang B, Lau YY, Liang M, Vainshtein I, Zusmanovich M, Lu H, *et al*. Mechanistic modeling of antigen sink effect for mavrilimumab following intravenous administration in patients with rheumatoid arthritis. J Clin Pharmacol. 2012;52(8):1150–61.
28. Lachmann HJ, Lowe P, Felix SD, Rordorf C, Leslie K, Madhoo S, *et al*. *In vivo* regulation of interleukin 1beta in patients with cryopyrin-associated periodic syndromes. J Exp Med. 2009;206(5):1029–36.
29. Hsei V, Deguzman GG, Nixon A, Gaudreault J. Complexation of VEGF with bevacizumab decreases VEGF clearance in rats. Pharm Res. 2002;19(11):1753–6.
30. Vugmeyster Y, DeFranco D, Szklut P, Wang Q, Xu X. Biodistribution of [125I]-labeled therapeutic proteins: application in protein drug development beyond oncology. J Pharm Sci. 2010;99(2):1028–45.
31. Lee JW, Kelley M, King LE, Yang J, Salimi-Moosavi H, Tang MT, *et al*. Bioanalytical approaches to quantify "total" and "free" therapeutic antibodies and their targets: technical challenges and PK/PD applications over the course of drug development. AAPS J. 2011;13(1):99–110.
32. Staack RF, Jordan G, Heinrich J. Mathematical simulations for bioanalytical assay development: the (un-)necessity and (im-)possibility of free drug quantification. Bioanalysis. 2012;4(4):381–95.